Korean J. of Chem. Eng., **10**(1), 18-27 (1993)

MATHEMATICAL MODELING OF BIO-PHYSICO CHEMICAL PROCESSES IN ACTIVATED CARBON COLUMNS

Sung Hyun Kim and Byoung Moo Min

Energy & Environment Research Department, Korea Institute of Energy Research,
P.O. Box 5, Taedok Science Town, Taejon 305-343, Korea
(Received 17 August 1992 • accepted 9 January 1993)

Abstract—Predictive mathematical models which describe the adsorption and biological phenomena in the plug-flow stationary solid phase column and completely mixed recycle fluidized bed were developed. The models incorporate liquid film transfer, biodegradation and diffusion in the biofilm, adsorption onto the adsorbent, as well as biofilm growth. The model equations are solved by a combination of orthogonal collocation and finite difference techniques. Computer simulations were conducted to compare the performance of the two models. Sensitivity tests were also performed to determine the effects of physical and biological parameters on model profiles.

INTRODUCTION

The role of activated carbon, applied to the removal of dissolved organic components has become paramount in water and wastewater treatment applications. Increasingly stringent water quality requirements have been sufficient incentives for environmental scientist and engineers to conceive novel and more efficient technologies for treatment of water and wastewater. Treatments based on physicochemical processes such as activated carbon adsorption have been considered technically viable for solving problems relating to water quality. However, major disadvantages of activated carbon application have been the high carbon cost, and significant thermal regeneration expenses associated with escalating energy costs.

Biological treatment systems have the potential to be relatively inexpensive for wastewater treatment. Interest in biological processes is increasing because they are economical, require low energy resources, and above all, convert toxic organic compounds to innocuous products such as carbon dioxide and water. The problems of biological processes are that they alone cannot remove non-biodegradable or slowly biodegradable organic pollutants. A promising method is the integration of activated carbon adsorption and biological degradation phenomena into a single unit. This combined process has several distinct advantages: (1) biodegradation of slowly biodegradable compounds by retention through adsorber beds [1]; (2) favorable environmental conditions for microorganism growth through enriched organic food and irregular surface area on activated carbon surface [2]: (3) protection of microorganism from toxic substances by activated carbon adsorption [3]; and, (4) elimination or dampening effect of concentration fluctuations of adsorbable compounds in the feed [4].

Although adsorption models which can predict the service life of activated carbon are relatively well developed, interaction with biodegradation causes considerable complications. A mathematical model capable of predicting the overall removal of dissolved organic matter (DOM) by a combined process of biodegradation and adsorption would therefore prove useful. Successful predictive mathematical models facilitate a better understanding of the various phenomena and mechanisms of interactions among microorganisms, substrate, and adsorbent, as well as provide the engineer with necessary design information. The principal objective of this work is two-fold: (1) establishing a basic theoretical framework which assesses adsorption and biodegradation behavior of a mixture of organic chemicals in biologically activated granular carbon (BAGC) systems; and (2) development of a model which can effectively predict those phenomena.

BACKGROUND

The substrate transport through the biofilm and into activated carbon particles is illustrated in Fig. 1. Bio-

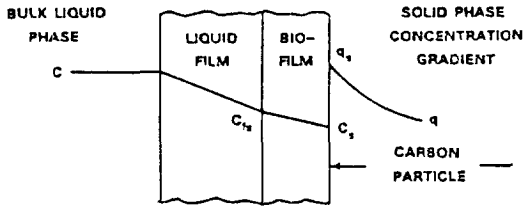

Fig. 1. Schematic representation of the essential components required to model a biofilm.

degradation and adsorption are unsteady-state processes taking place during the service life of carbon bed. Major factors influencing the rate of each process are: transport of materials in the liquid phase, microbial growth kinetics (and thus the microbial biodegradation rate), intraparticle transport kinetics, and adsorption onto the solid phase.

Extensive studies have been conducted to develop mathematical models which take into consideration the above-mentioned factors for fixed, expanded or fluidized activated carbon beds [4-9]. A literature review reveals several modeling efforts which incorporate biological activity in activated carbon adsorber models. Jennings [5] investigated the removal of biodegradable compounds by attached film growth and presented a phenomenological analysis in terms of simultaneous diffusion and chemical reaction of the species across the biofilm. His model essentially employed a lumped-parameter approach, representing the concentration of the organic species as total organic carbon (TOC). His steady-state model for biological utilization of substrate was effective in predicting steady state substrate removals in the case of glucose and sodium lactate. There was no necessity to incorporate a rigorous description of adsorption dynamics for his specific system since glucose and sodium lactate manifest poor adsorbabilities on activated carbon. Extrapolation of this model to treatment processes integrating adsorption and biodegradation for specific wastewater applications would however require a rigorous description of adsorption dynamics and transport for achieving better predictions of effluent concentration porfiles.

The mathematical conceptualization of Jennings was extended by Peel and Benedek [6] whose predictive model assumed plug-flow conditions, with the carbon particles held in stationary positions in the adsorber column. An additional assumption was that film thickness was considered as a fixed, externally defined parameter. This approximation worked reasonably well for prediction of long-term performance of their system, although higher removals were predicted at the initial stages of column operation, as demonstrated by the investigators. This might be attributed to the fact that, at the commencement of the operation cycle the biofilm is very thin, and as time progresses, the film thickness increases. It was therefore necessary to develop a model that considered the spatial and temporal variations of biofilm thickness in adsorbers.

Ying and Weber [4] responded to the above-mentioned need by conceptualizing a model, in which the film thickness in an adsorber was a function of both time and distance into the bed. Their model included the phenemenological aspects of liquid film transfer, intraparticle diffusion, substrate utilization by Monod kinetics, and build-up of biomass. In their model, the bacterial films were allowed to grow until they reached a certain level, whereafter they were maintained at this externally defined thickness by washing and air-scouring the bed. The actual film thickness was assumed to correspond to less than that of a monolayer of bacteria, and consequently, no allowance was made to account for the additional external mass transfer resistance to adsorption due to intra-biolayer diffusion. The model was applicable to both plug-flow column and completely mixed fluidized bed adsorbers, and was found to have good predictive capability in the case of glucose and sucrose.

Andrews and Tien [7] presented a biological model for fluidized bed based on the completely mixed reactor assumption for both liquid phase and carbon particles. The important phenomenological assumptions employed in model development included the following: (1) mass transfer resistance of the external liquid film and diffusion resistance of the internal solid phase were considered negligible; (2) the organic substrate was assumed to be present in low concentration to limit bacterial growth; and (3) to facilitate and analytical solution, uptake of organic substrate by the biofilm was assumed to follow first-order kinetics, and the equations pertaining to the model were solved for a quasi steady-state condition. The model exhibited good capability to predict effluent profiles for their specific organic substrate (valeric acid) at dilute concentrations. In order to enlarge the domain of applicability of the model to treatment of real wastewaters having diverse compositions and manifesting system-specific characteristics, a few important aspects have to be considered. It would be more appropriate to assume that substrates might be present in high concentrations, and that the resistance to mass transfer due to liquid film diffusion should not be neglected. Furthermore, a model had to be developed that would

be suitable for prediction of performances of plug-flow adsorbers as well.

Recently, two other groups of researchers, namely, DiGiano et al. [8], and Chang and Rittmann [9], have proposed similar models based on the fundamental mechanisms of film transport, biodegradation within the biofilm, adsorption within the activated carbon, and growth of biofilm. The model proposed by Chang and Rittmann is a logical extension of that attributed to DiGiano and coworkers, although there are a few important differences between them. The former model has been formulated for a completely mixed reactor, while the latter has been developed for an infinite bath configuration. Furthermore, the initial conditions used in these models are different. These models were intended to be applied for relatively low single substrate concentrations. They proved to be effective in predicting removal efficiencies of phenol, an easily biodegradable substrate.

The model proposed in this paper incorporates a number of features to obviate the limitations of previous models for organic carbon removal. The model provides a rigorous description of adsorption dynamics, considers external mass transfer, internal diffusion transport, intra-biofilm diffusion, and above all, spatial and temporal variation of biofilm thickness in adsorbers. Furthermore, the model is applicable to plug-flow column as well as completely mixed fluidized bed designs, and is intended to be applied to actual water and wastewaters with radically different total organic carbon (TOC) levels, and components manifesting varying adsorption or biodegradation characteristics.

MODEL DEVELOPMENTS

The first step in the development of any conceptual model involves its reduction to essential components. Fig. 1 shows the schematic of essential components required to model biofilm transport and carbon adsorption of substrate. As illustrated, microorganisms in a biofilm with density X_f get attached to an activated carbon surface and grow as the sorptive capacity within the carbon particle becomes exhausted. During its initial phase of development, the biofilm is very thin and much of the substrate is transported to the granular activated carbon (GAC) surface where adsorption occurs. The model is based on the fundamental mechanisms of transport of substrate in the liquid phase, transport and degradation within the biofilm, adsorption within the activated carbon, and growth of the biofilm. This model is conceptually similar to

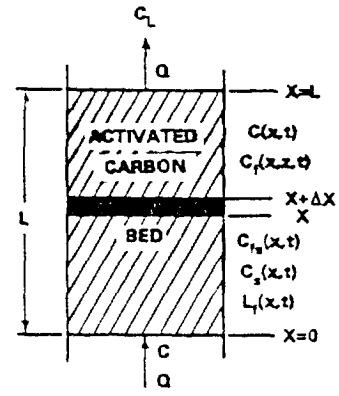

Fig. 2. Schematic representation of an activated carbon bed.

those of DiGiano et al. [8], and Chang and Rittmann [9], although it differs from the completely mixed fluidized model of Chang and Rittmann in that it takes into account the variation of concentration as a function of axial position in the bed. Furthermore, this model employs different initial and boundary conditions.

In this research, two different model were developed for general applicability to water and wastewater treatment. These include plug-flow stationary solid phase activated carbon columns and completely mixed recycle fluidized beds. In order to develop a realistic mathematical model, it is not possible to consider every phenomenon which occurs in the biofilm and activated carbon phase. Reasonable assumptions have therefore been made for the purpose of simplifying complex physical and biological phenomena. In both plug-flow stationary solid phase columns (PSSPC) and completely mixed recycle fluidized beds (CMRFB), bacterial growth causes particle enlargement and the associated implications affect liquid flow patterns and solid mixing. The bacterial growth also results in an increase in the pressure drop necessary to maintain a constant flow rate or an increase in the bed height, and thus makes modeling particularly difficult for predicting long-term operations. During the early stages of column run, an assumption required for model development is that the change of bed porosity due to bacterial growth is negligible. The conceptual mechanism of the models are embodied in Figs. 2 and 3. The following assumptions are incorporated for simplification of mathematical analysis:

(1) Axial dispersion for the liquid phase is considered;

(2) The column has uniform cross section and the

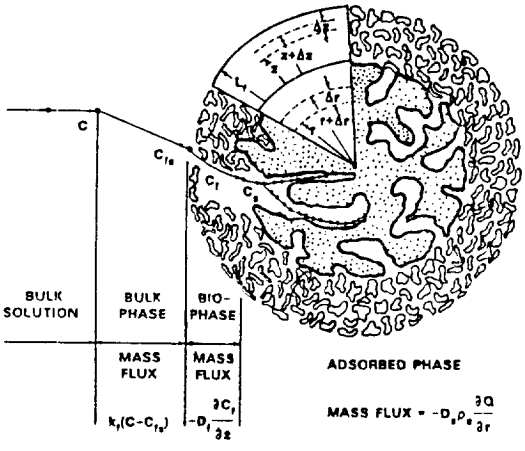

Fig. 3. Conceptual model of biofilm attached to an activated carbon particle and supplied by substrate from both external solution phase and internal adsorbent particle.

adsorbent granules are spherical and of uniform size;

(3) Contribution of pore diffusion to the adsorbate transport has been neglected because surface diffusion flux is much larger than pore-diffusion flux;

(4) The biofilm is homogeneous; i.e., its porosity, bacterial density, composition, etc., do not vary with film thickness;

(5) Organic substrate is soluble, biodegradable and adsorbable;

(6) The substrate concentration profile across the bacterial film outside adsorbents can be considered to be in a pseudo steady-state even though the film thickness changes with time;

(7) The biological activity is assumed to be substrate-limiting, and its kinetics are presented by the Monod equation;

(8) Bacterial activity in the liquid phase is negligible;

(9) The desorption of adsorbed substrate does not occur.

Case 1. PSSPC Model

1-1. Liquid Phase Material Balance

The material balance of the dissolved substrates to be removed for any differential segment of the bed is represented by the equation

$$\frac{\partial C(x,t)}{\partial t}=D_d\frac{\partial^2 C(x,t)}{\partial x^2}-v_s\frac{\partial C(x,t)}{\partial x}-\frac{3k_f(1-\varepsilon)}{\varepsilon}\frac{(R+L_f)^2}{R^3}[C(x,t)-C_{fs}(x,t)] \quad (1)$$

whose initial and boundary conditions are

$$C(x,t=0)=0 \quad (2)$$

$$C(x=0,t)=C_o \quad (3)$$

$$\left.\frac{\partial C(x,t)}{\partial x}\right|_{x=L}=0 \quad (4)$$

1-2. Solid Phase Material Balance in the Adsorbent

The homogeneous surface diffusion model used for intraparticle diffusion of adsorbed substrate can be represented by

$$\frac{\partial q(r,t)}{\partial t}=\frac{D_s}{r^2}\frac{\partial}{\partial r}\left[r^2\frac{\partial q(r,t)}{\partial r}\right] \quad (5)$$

whose initial and boundary conditions are

$$q(0\le r\le R,\ t=0)=0 \quad (6)$$

$$q(r=R,\ t)=q_s(t) \quad (7)$$

$$\frac{\partial q(r=0,\ t\ge t_o)}{\partial r}=0 \quad (8)$$

Another boundary condition can be introduced by performing mass balance on an adsorbent particle as shown below:

$$\frac{3}{R^3}\frac{\partial}{\partial t}\int_0^R q(r,t)r^2\,dr=\frac{k_fA_p}{V_s\rho_a}[C(x,t)-C_{fs}(x,t)]-\frac{3kX_fL_f}{Y\rho_aR}\frac{C_{favg}(x,t)}{K_s+C_{favg}(x,t)} \quad (9)$$

1-3. Diffusion and Reaction in the Biofilm

Assuming that substrate concentration within the biofilm changes only in the z direction, normal to the surface of the biofilm, and that substrate concentration profile across the biofilm is at pseudo steady-state, the following relation can be written:

$$D_f\frac{\partial^2 C_f(x,z,t)}{\partial z^2}=\frac{kX_fC_f(x,z,t)}{K_s+C_f(x,z,t)} \quad (10)$$

The boundary conditions corresponding to the above equation are the following:

$$C_f(x,z=0,t)=C_s(x,t) \quad (11)$$

$$C_f(x,Z=L_f,t)=C_{fs}(x,t) \quad (12)$$

1-4. Growth of Biofilm

If the Monod growth model is used, the variation of biofilm thickness with time can be adequately represented by

$$\frac{\partial L_f(x,t)}{\partial t}=\frac{kC_{favg}(x,t)L_f(x,t)}{K_s+C_{favg}(x,t)}-K_dL_f(x,t) \quad (13)$$

The initial and boundary condition are

$$L_f(x,t=0)=L_{fo} \quad (14)$$

$$L_f(x, t=t_{max}) = L_{fmax} \tag{15}$$

1-5. Adsorption Equilibrium Relationship

The Freundlich adsorption model used to relate the equilibrium solid phase concentration to liquid phase concentration near the exterior particle surface can be written as

$$q(r=R, x, t) = K_f C_s(x, t)^n \tag{16}$$

Non-dimensionalization of variables is an important aspect to be considered with regard to applications of numerical techniques. It is convenient to normalize the domains of variables (often between zero and unity), and express differential equations and their initial and boundary conditions in a systematized and compact form. Furthermore, the transformation process renders the equations more easily amenable to techniques such as orthogonal callocation, facilitates a better analysis of system characteristics from values of dimensionless groups, and provides more information on convergence, consistency, and stability properties of the numerical scheme employed.

Eqs. (1) through (16) can be non-dimensionalized by defining the following dimensionless variables:

$$\bar{C} = \frac{C}{C_o} \tag{17}$$

$$\bar{C}_s = \frac{C_s}{C_o} \tag{18}$$

$$\bar{C}_{fs} = \frac{C_{fs}}{C_o} \tag{19}$$

$$\bar{C}_f = \frac{C_f}{C_o} \tag{20}$$

$$\bar{C}_{favg} = \frac{C_{favg}}{C_o} \tag{21}$$

$$\bar{q} = \frac{q}{q_o} \tag{22}$$

$$\bar{L}_f = \frac{L_f}{L_{fmax}} \tag{23}$$

$$\bar{x} = \frac{x}{L} \tag{24}$$

$$\bar{z} = \frac{z}{L_f} \tag{25}$$

$$\bar{r} = \frac{r}{R} \tag{26}$$

Then the system of equations representing the model can be transformed by non-dimensionalization as shown below:

$$\frac{\partial \bar{C}(\bar{x}, T)}{\partial T} = D_d \frac{\partial^2 \bar{C}(\bar{x}, T)}{\partial \bar{x}^2} - D_g \frac{\partial \bar{C}(\bar{x}, T)}{\partial \bar{x}} - 3D_g S_t (1 + B_o \bar{L}_f)^2 [\bar{C}(\bar{x}, T) - \bar{C}_{fs}(\bar{x}, T)] \tag{27}$$

$$\frac{\partial \bar{q}(\bar{r}, \bar{x}, T)}{\partial T} = \frac{E_d}{\bar{r}^2} \frac{\partial}{\partial \bar{r}} \left[\bar{r}^2 \frac{\partial \bar{q}(\bar{r}, \bar{x}, T)}{\partial \bar{r}} \right] \tag{28}$$

$$\frac{\partial}{\partial T} \int_0^1 \bar{q}(\bar{r}, \bar{x}, T) \bar{r}^2 d\bar{r} = S_t (1 + B_o \bar{L}_f)^2 [\bar{C}(\bar{x}, T) - \bar{C}_{fs}(\bar{x}, T) - A_1 D_g \frac{\bar{L}_f(\bar{x}, T) \bar{C}_{favg}(\bar{x}, T)}{B_1 + \bar{C}_f(\bar{x}, T)} \tag{29}$$

$$\frac{\partial^2 \bar{C}_f(\bar{x}, \bar{z}, T)}{\partial \bar{z}^2} = A_2 \frac{\bar{L}_f^2(\bar{x}, T) \bar{C}_f(\bar{x}, \bar{z}, T)}{B_1 + \bar{C}_f(\bar{x}, \bar{z}, T)} \tag{30}$$

$$\frac{\partial \bar{L}_f(\bar{x}, T)}{\partial T} = A_3 D_g \frac{\bar{C}_{favg}(\bar{x}, T) \bar{L}_f(\bar{x}, T)}{B_1 + \bar{C}_{favg}(\bar{x}, T)} - A_3 D_g \bar{L}_f(\bar{x}, T) \tag{31}$$

$$\bar{q}(\bar{r}=1, \bar{x}, T) = \bar{C}_s(\bar{x}, T)^n \tag{32}$$

where dimensionless parameters and defined as follows:

$$D = D_g D_k \tag{33}$$

$$D_g = \frac{\rho_a q_o (1-\varepsilon)}{\varepsilon C_o} \tag{34}$$

$$D_k = \frac{D_d \tau}{L^2} \tag{35}$$

$$S_t = \frac{k_f \tau (1-\varepsilon)}{R\varepsilon} \tag{36}$$

$$B_o = \frac{L_{fmax}}{R} \tag{37}$$

$$B_1 = \frac{K_s}{C_o} \tag{38}$$

$$E_d = \frac{D_s D_g \tau}{R^2} \tag{39}$$

$$A_o = \frac{Q\tau(1-\varepsilon)}{3V_r \varepsilon} \tag{40}$$

$$A_1 = \frac{k\tau X_f L_{fmax}}{Y q_o \rho_a R} \tag{41}$$

$$A_2 = \frac{k X_f L_{fmax}^2}{C_o D_f} \tag{42}$$

$$A_3 = k\tau \tag{43}$$

$$T = \frac{t}{\tau D_g} \tag{44}$$

$$\tau = \frac{L}{V_x} \tag{45}$$

$$q_o = K_F C_o^n \tag{46}$$

$$v_x = \frac{Q}{A} \tag{47}$$

The initial and boundary conditions in dimensionless form are:

$$\bar{C}(\bar{x}, T=0) = 0 \tag{48}$$

$$\bar{C}(\bar{x}=0, T) = 1 \tag{49}$$

$$\frac{\partial \bar{C}(\bar{x}, T)}{\partial \bar{x}}\Big|_{\bar{x}=1} = 0 \tag{50}$$

$$\bar{q}(r, T=0) = 0 \tag{51}$$

$$\frac{\partial \bar{q}(\bar{r}=0, T)}{\partial \bar{r}} = 0 \tag{52}$$

$$\bar{C}_f(\bar{x}, \bar{z}=0, T) = \bar{C}_s(\bar{x}, T) \tag{53}$$

$$\bar{C}_f(\bar{x}, \bar{z}=1, T) = \bar{C}_{fs}(\bar{x}, T) \tag{54}$$

$$\bar{L}_f(\bar{x}, T=0) = \bar{L}_{fo} \tag{55}$$

$$\bar{L}_f(\bar{x}, T=T_{max}) = 1 \tag{56}$$

Case 2. CMRFB Model

In this case, Eqs. (1) through (16) remain as in PSSPC of Case 1, describing the liquid phase material balance, solid phase diffusion in the adsorbent, diffusion and reaction in the biofilm, growth of biofilm and adsorption isotherm model, respectively. However, the boundary conditions of Eqs. (3) and (9) are different from those of the PSSPC model. Eq. (3) is hence replaced by

$$C(x, t)|_{x=0} = \frac{QC_o + Q_r C}{Q + Q_r} \tag{57}$$

When the liquid phase substrate removal is negligible, the boundary condition of Eq. (9) can be replaced by performing mass balance on an adsorbent particle as shown below:

$$\frac{3}{R^3}\frac{\partial}{\partial t}\int_0^R q(r, t) r^2\, dr = \frac{Q}{V_c \rho_a}[C_o - C(x, t)|_{x=L}] - \frac{3kX_f L_f}{YR\rho_a}\frac{C_{favg}(x, t)}{K_s + C_{favg}(x, t)} \tag{58}$$

The dimensionless system of equations which describe the CMRFB model are the following:

$$\frac{\partial \bar{C}(\bar{x}, T)}{\partial T} = D\frac{\partial^2 \bar{C}(\bar{x}, T)}{\partial \bar{x}^2} - D_g\frac{\partial \bar{C}(\bar{x}, T)}{\partial \bar{x}} - 3D_g S_f(1 + B_o \bar{L}_f)^2[\bar{C}(\bar{x}, T) - \bar{C}_{fs}(\bar{x}, T)] \tag{59}$$

$$\frac{\partial \bar{q}(\bar{r}, \bar{x}, T)}{\partial T} = \frac{E_d}{\bar{r}^2}\frac{\partial}{\partial \bar{r}}\left[\bar{r}^2\frac{\partial \bar{q}(\bar{r}, \bar{x}, T)}{\partial \bar{r}}\right] \tag{60}$$

$$\frac{\partial}{\partial T}\int_0^1 \bar{q}(\bar{r}, \bar{x}, T)\bar{r}^2\, d\bar{r} = A_o[1 - \bar{C}(\bar{x}, T)|_{\bar{x}=1}] - A_1 D_g \frac{\bar{L}_f(\bar{x}, T)\bar{C}_{favg}(\bar{x}, T)}{B_1 + \bar{C}_{favg}(\bar{x}, T)} \tag{61}$$

$$\frac{\partial^2 \bar{C}_f(\bar{x}, \bar{z}, T)}{\partial \bar{z}^2} = A_2\frac{\bar{L}_f^2(\bar{x}, T)\bar{C}_f(\bar{x}, \bar{z}, T)}{B_1 + \bar{C}_f(\bar{x}, \bar{z}, T)} \tag{62}$$

$$\frac{\partial \bar{L}_f(\bar{x}, T)}{\partial T} = A_3 D_g \frac{\bar{C}_{favg}(\bar{x}, T)\bar{L}_f(\bar{x}, \bar{z}, T)}{B_1 + \bar{C}_{favg}(\bar{x}, T)} - A_3 D_g \bar{L}_f(\bar{x}, T) \tag{63}$$

$$\bar{q}(r=1, \bar{x}, T) = \bar{C}_s(\bar{x}, T)^n \tag{64}$$

All dimensionless parameters and variables in Eqs. (17) through (26), and (33) through (46) are defined as they were for the case of PSSFC model, with the exception of Eq. (47), which is replaced in the completely mixed recycle fluidized bed model by the relation

$$v_x = \frac{Q + Q_r}{A} \tag{65}$$

The initial and boundary conditions are:

$$\bar{C}(\bar{x}=0, T) = 0 \tag{66}$$

$$\frac{\partial \bar{C}(\bar{x}, T)}{\partial \bar{x}}\Big|_{\bar{x}=1} = 0 \tag{67}$$

$$\bar{q}(\bar{r}, T=0) = 0 \tag{68}$$

$$\frac{\partial \bar{q}(\bar{r}=0, T)}{\partial \bar{r}} = 0 \tag{69}$$

$$\bar{C}_f(\bar{x}, \bar{z}=0, T) = \bar{C}_s(\bar{x}, T) \tag{70}$$

$$\bar{C}_f(\bar{x}, \bar{z}=1, T) = C_{fs}(\bar{x}, T) \tag{71}$$

$$\bar{L}_f(\bar{x}, T=0) = \bar{L}_{fo} \tag{72}$$

$$\bar{L}_f(\bar{x}, T=T_{max}) = 1 \tag{73}$$

NUMERICAL SOLUTION

A number of numerical techniques are available which can be employed to solve these equations. In this study, a combined technique of orthogonal collocation and finite difference methods was employed to obtain long-term predictions of effluent concentration profiles for the PSSPC and CMRFB systems. The general philosophy behind application of orthogonal collocation is the reduction of a complicated system of partial differential equations to a more tractable system of ordinary differential equations. Orthogonal collocation method was used to solve partial differential Eqs. (27), (28) and (29), and finite difference method, for Eqs. (30) and (31).

The application of orthogonal collocation to Eq. (27) results in the following ordinary differential equation:

$$\frac{d\bar{C}_k}{dT} = D\sum_{j=1}^{M_c} BU_{i,j}\bar{C}_j - D_g\sum_{j=1}^{M_c} AU_{ij}\bar{C}_j - 3D_gS_t(1+B_o\bar{L}_f)^2(\bar{C}_k-\bar{C}_{fs,k}) \quad (k=2, M_c) \quad (74)$$

The subscript i represents a collocation point in the axial direction and the matrices AU and BU represent collocation constants for first and second order derivatives determined from the roots of the assymmetric Legendre polynomials as discussed by Finlayson [10].

Application of orthogonal collocation transforms Eq. (31) to the following ordinary differential equation:

$$\frac{d\bar{q}_{i,k}}{dT} = E_d\sum_{j=1}^{M_c} B_{i,j}\bar{q}_{j,k} \quad (i=1, N_c;\ k=1,\ M_c) \quad (75)$$

The subscript counter i represents a collocation point in the radial direction, and as previously noted, the subscript counter k represents the axial position. Adsorbent-phase concentrations, $q_{i,k}$ are matrices that represent unknowns resulting from the application of orthogonal collocation in the radial direction on Eq. (75), and in the axial direction on Eq. (74). Matrix B represents the set of collocation constants for the Laplacian operator with spherical geometry, and its elements are determined from the roots of symmetric Legendre polynomials as discussed earlier [10]. The application of orthogonal collocation to Eqs. (29) and (61) results in the following relation involving the adsorbent phase for PSSFC system:

$$\frac{d\bar{q}_{N_c,k}}{dT} = \left[S_t(1+B_o\bar{L}_{f,k})^2(\bar{C}_k-\bar{C}_{fs,k}) - A_1D_g\frac{\bar{L}_{f,k}\bar{C}_{favg,k}}{B_1+\bar{C}_{favg,k}} - \sum_{j=1}^{N_c-1} W_j\frac{d\bar{q}_{j,k}}{dT}\right]\frac{1}{W_{N_c}} \quad (76)$$

For CMRFB, the above equation takes the form

$$\frac{d\bar{q}_{N_c,k}}{dT} = \left[A_o(1-\bar{C}_k) - A_1D_g\frac{\bar{L}_{f,k}\bar{C}_{favg,k}}{B_1+\bar{C}_{favg,k}} - \sum_{j=1}^{N_c-1} W_j\frac{d\bar{q}_{j,k}}{dT}\right]\frac{1}{W_{N_c}} \quad (77)$$

The subscript N_c refers to the adsorbent-phase concentration at the surface and the subscript k refers to the axial position. The weighting factors, W_j, used for integration, are determined from the roots of symmetric Legendre polynomials [10]. Eqs. (76) and (77) are valid throughout the bed, or from k+1 to M_c.

The dimensionless biofilm diffusion equation was solved using the finite difference method. For diffusion and reaction in the biofilm represented by Eq. (30), the finite difference approximation is

$$\frac{\bar{C}_{f,m+1,k}-2\bar{C}_{f,m,k}+\bar{C}_{f,m-1,k}}{\Delta\bar{z}^2} = A_2\frac{\bar{L}_f^2\bar{C}_{f,m,k}}{B_1+\bar{C}_{f,m,k}} \quad (78)$$

For the growth of biofilm represented by Eq. (31), the relation is

$$\bar{L}_{f,j+1,k} = \bar{L}_{f,j,k}\left[1+\Delta T\left(\frac{A_3D_g\bar{C}_{favg,k}}{B_1+\bar{C}_{favg,k}}\right)\right] - A_3D_g \quad (79)$$

Biofilm thickness is divided into (m+1) finite points. $\bar{C}_{f,1,k}$ and $\bar{C}_{f,2,k}$ are calculated from the equations

$$\bar{C}_{f,1,k} = 2\bar{C}_{s,k} + \frac{A_2\bar{L}_{f,k}}{\Delta\bar{z}^2}\frac{\bar{C}_{s,k}}{B_1+\bar{C}_{s,k}} \quad (80)$$

$$\bar{C}_{f,2,k} = 2\bar{C}_{f,1,k} - \bar{C}_{s,k} + \frac{A_2\bar{L}_{f,k}}{\Delta\bar{z}^2}\frac{\bar{C}_{f,1,k}}{B_1+\bar{C}_{f,1,k}} \quad (81)$$

$\bar{C}_{f,m+1,k}$ is obtained by substituting for $\bar{C}_{f,1,k}$ and $\bar{C}_{f,2,k}$ into Eq. (70), and $\bar{C}_{favg,k}$ is determined from the following equation:

$$\bar{C}_{favg,k} = (\bar{C}_{s,k} + \sum_{j=1}^{m+1}\bar{C}_{f,i,k})/(m+1) \quad (82)$$

$\bar{C}_{favg,k}$ is then substituted into Eq. (79) to obtain $\bar{L}_{f,k,j+1}$ at each time step. The final equation needed for the model is the Freundlich coupling equation

$$\bar{q}_{N_c,k} = \bar{C}_{s,k}^{\ n} \quad (83)$$

valid for k=1 to M_c.

The number of ordinary differential equations generated by application of orthogonal collocation to axial and radial directions are M_c-1 in the liquid phase, and N_c*M_c in the adsorbent phase, respectively. It was found that seven internal collocation points in the radial direction and eight in the axial direction provided excellent numerical accuracy. Seven ordinary differential equations for the liquid phase, and fifty-six for the adsorbent phase were required, and a total of sixty three ordinary differential equations were solved using the algorithm developed by GEAR [11].

SIMULATIONS

The two mathematical models thus developed predict the dynamics of bioactive adsorbers of plug-flow stationary solid phase column (Model A) and completely mixed recycle fluidized bed (Model C). Further, in order to assess biofilm diffusion resistance effect on adsorption rate, Model A was modified following the assumption of no resistance due to biofilm (Model B). To accomplish this, Eq. (30) was neglected and the remaining equations solved using the same numerical technique. Table 1 summarizes model conditions and

Table 1. Predictive mathematical models for biologically activated carbon adsorbers

Model designation	Conditions	Biofilm resistance effect
A	Plug-flow stationary solid phase column	Yes
B	Plug-flow stationary solid phase column	No
C	Completely mixed solid phase recycle fluidized bed	Yes

Table 2. Common input parameters for model sensitivity

Input parameters	Values	Input parameters	Values
W(g)	5.96	$D_f(cm^2/sec)$	4.48×10^{-6}
DIA(cm)	1.0	$k(min^{-1})$	6.67×10^{-3}
C_o(mg/L)	80	Y(mg/mg)	1.25
Q(mL/min)	6.5	K_s(mg/L)	125
L(cm)	17.5	$K_d(min^{-1})$	5×10^{-5}
R(cm)	0.0179	$X_f(mg/cm^3)$	31
K_F	11.48	$L_{f0}(\mu m)$	1.0
n	0.423	$L_{fmax}(\mu m)$	60
$D_s(cm^2/sec)$	1×10^{-6}	$D_d(cm^2/sec)$	114.0
k_f(cm/sec)	1.74×10^{-3}	R_{ec}	25
$D_f(cm^2/sec)$	5.6×10^{-6}		

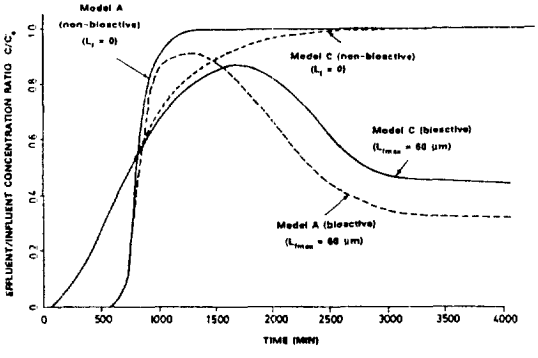

Fig. 4. Comparison of effluent concentrations for PSSPC and CMRFB models.

designation.

Model simulations were conducted to investigate the system performance, as well as effects of influencing parameters. The input parameters listed in Table 2 were used in the simulations. They were estimated from literature data [12-14].

A comparison of the performances of the PSSPC model (Model A) and CMRFB model (Model C) for

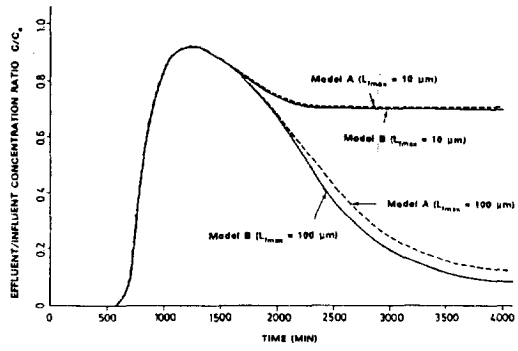

Fig. 5. Comparison of breakthrough profiles depicting effects of biofilm thickness.

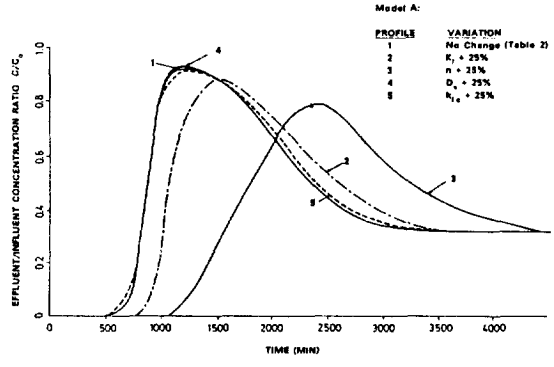

Fig. 6. Model sensitivity of variations in Freundlich isotherm parameters, K_f and n, and mass transfer coefficients k_{fc} and D_s.

bioactive and non-bioactive adsorbers is presented in Fig. 4. The results are given in the form of effluent concentration vs. time for a given bed height. The effluent profile for adsorption without biological activity was obtained as a limiting case by substituting a zero value for biofilm thickness ($L_f=0$) into Models A and C. As may be observed, substantial differences between the two model profiles exist. Faster breakthrough and a significantly higher steady-state effluent concentration is observed in the case of CMRFB.

Fig. 5 illustrates the effect of biofilm thickness on effluent concentration profiles for Models A and B. The simulation results indicate that the effect of biofilm thickness is insignificant at 10 μm, and becomes slightly more pronounced as the thickness is increased. It can therefore be concluded that biofilm diffusion resistance may be disregarded for such systems. This is in accord with the assumption made by Ying and Weber [4] in their model development.

Finally, three sets of simulation analyses were conducted to test the sensitivity of models with respect

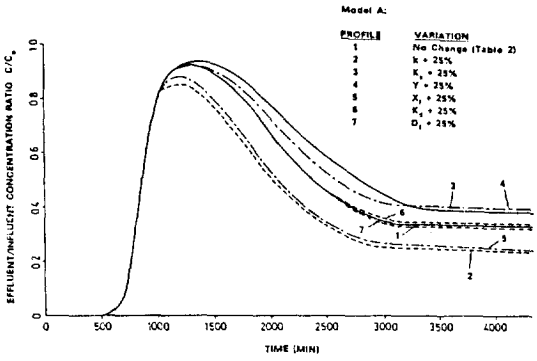

Fig. 7. Model sensitivity to variations in biological parameters, k, K_s, Y, X_f, K_d and D_f.

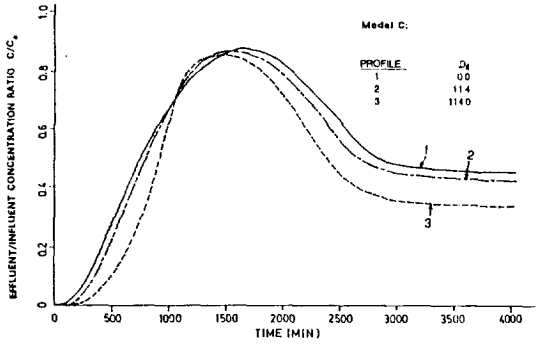

Fig. 8. Model profiles for variations in axial dispersion coefficient, D_d.

to: (1) adsorption isotherm parameters, K_F and n, and mass transfer parameters, k_{fc} and D_s, for Model A, shown in Fig. 6; (2) biological parameters k, K_s, Y, X_f, K_d and D_f for Model A, presented in Fig. 7; (3) axial dispersion parameter, D_d for Model C, illustrated in Fig. 8. Breakthrough profiles designated 2, 3, 4 and 5 in Fig. 6 are model profiles for a 25 percent increase in the values of K_F, n, k_{fc}, and D_s, respectively. As may be observed, variations of the Freundlich isotherm parameters, K_F and n, strongly affect the breakthrough simulation profiles, especially the exponential parameter. The film transfer coefficient, k_{fc} and intraparticle surface diffusion coefficient, D_s, have no significant effect on effluent concentrations.

Results of sensitivity studies for the biological parameters, k, K_s, Y, X_f, K_d, and D_f are depicted in Fig. 7. A careful examination of the simulation profiles indicates that the effluent profiles are more sensitive to the Monod kinetic constants, biomass yield, and biomass concentration in the biofilm. The profiles are relatively insensitive to biomass decay coefficient and biofilm diffusivity.

The effects of variations in axial dispersion coefficient, D_d, of fluidized bed on effluent concentration are illustrated in Fig. 8. As evident, the significant changes are observed with regard to variations in axial dispersion coefficient.

Based on the simulation results, a systematic laboratory experimentation program was designed and executed to verify the PSSPC and CMRFB model predictions with experimental results [15].

CONCLUSIONS

Mathematical models for PSSPC and CMRFB were developed and simulated using model parameters of Table 2. The major findings are summarized below:

1. A comparison of PSSPC and CMRFB models showed substantial differences in their breakthrough profiles. Faster breakthrough was observed in the case of the CMRFB model.

2. Model simulations indicate that biofilm thickness does not pose significant resistance to mass transfer, and thus may be disregarded in such systems.

3. The simulation studies reported herein have shown that adsorption and transport parameters characterized by K_F, n, k_{fc} and D_s, strongly affect the initial stages of breakthrough curves, while biological parameters characterized by k, K_s, Y, X_f and K_d control steady-state effluent concentrations. The effects of variations in axial dispersion coefficient, D_d, appear to have a significant effect on effluent concentrations.

NOMENCLATURE

A : cross section area [L^2]
A_p : total surface area available for mass transfer [L^2]
a : surface area per particle [L^2]
AU : unsymmetric second order collocation constant
B : symmetric second order collocation constant
BU : unsymmetric first order collocation constant
C : substrate concentration in liquid phase [M_s/L^3]
C_f : substrate concentration in biofilm [M_s/L^3]
C_{favg} : average substrate concentration in biofilm [M_s/L^3]
C_{fs} : substrate concentration at biofilm/liquid interface [M_s/L^3]
C_o : influent substrate concentration [M_s/L^3]
C_s : substrate concentration near activated carbon surface [M_s/L^3]
D_d : axial dispersion coefficient [L^2/T]
D_f : substrate diffusion coefficient in biofilm [L^2/T]
D_s : substrate diffusion coefficient in activated carbon

$[L^2/T]$

DIA : diameter of the activated carbon column [L]

k : maximum specific substrate utilization rate $[M_s/(M_x T)]$

k_{fc} : liquid film transfer coefficient in column study [L/T]

K_d : overall biofilm loss coefficient [1/T]

K_F : Freundlich isotherm constant $[(M_s/M_q)(L^3/M_s)^n]$

K_s : Monod half saturation coefficient $[M_s/L^3]$

L : length of activated carbon fluidized bed [L]

L_f : biofilm thickness [L]

L_{f0} : initial biofilm thickness [L]

L_{fmax} : maximum biofilm thickness [L]

m : number of finite points in the biofilm

M_c : number of internal collocation points in the axial direction

n : Freundlich isotherm constant

N_c : number of internal collocation points in the radial direction

q : sorbed phase substrate concentration $[M_s/M_q]$

Q : influent flow rate $[L^3/T]$

Q_r : recirculation flow rate $[L^3/T]$

r : radial coordinate in activated carbon particle [L]

R : radius of activated carbon particle [L]

R_{ec} : recycle ratio (dimensionless)

t : time [T]

t_{max} : time corresponding to maximum film thickness L_{fmax} [T]

t_0 : initial time [T]

T_{max} : dimensionless time corresponding to t_{max}

ΔT : dimensionless increment for time

v_x : interstitial axial fluid velocity [L/T]

V_c : total activated carbon volume in the bed $[L^3]$

W : weighting factors for collocation integration of the symmetric Legendre polynomials

WT : weight of activated carbon in adsorber $[M_q]$

x : coordinate for axial position in activated carbon bed [L]

X_f : biomass density in biofilm $[M_x/L^3]$

Y : microbial yield coefficient $[M_x/M_s]$

z : coordinate for position in biofilm [L]

$\Delta\bar{z}$: dimensionless increment for position z in biofilm

Greek Letters

ρ_a : apparent density of activated carbon $[M_q/L^3]$

ε : fraction of volumetric space unoccupied by activated carbon

τ : empty bed contact time [T]

where units symbols are

L : length

M_q : mass of activated carbon

M_s : mass of substrate

M_x : mass of microorganisms

T : time

REFERENCES

1. Schultz, J. R. and Keinath, T. M.: *WPCF.*, **56**(2), 143 (1984)
2. den Blanken, J. G.: *Environ. Eng. Div., ASCE.*, **108** (2), 405 (1982)
3. Nayar, S. C. and Sylvester, N. D.: *Water Res.*, **13**(2), 201 (1979).
4. Ying, W. and Weber, W. J., Jr.: *WPCF.*, **51**(11), 2661 (1979).
5. Jennings, P. A.: Ph.D. Dissertation, University of Illinois, Urbana-Champaign, (1975).
6. Peel, R. and Benedek, A.: *AIChE Sym. Ser.*, **73** (166), 25 (1975).
7. Andrews, G. F. and Tien, C.: *AIChE J.*, **27**(3), 396 (1981).
8. DiGiano, F. A., Dovantzis, K. and Speitel, G. E., Jr.: Proc. National Conf. on Environ. Eng., ASCE., 382 (1984).
9. Chang, H. T. and Rittmann, B. E.: *Environ. Sci. Tech.*, **21**(3), 273 (1987).
10. Finlayson, B. A.: "The Method of Weighted Residuals and Variational Principles", Academic Press, New York, NY (1972).
11. Gear, C. W.: "Numerical Initial Value Problems in Ordinary Differential Equations", Prentice-Hall, Englewood Cliffs, N. J.(1976).
12. Peil, K. H. and Gaudy, A. F., Jr.: *Applied Microbiology*, **21**(2), 253 (1971).
13. Ying, W.: Ph.D. Dissertation, The University of Michigan, Ann Arbor, Mich.(1978).
14. Rittmann, B. E. and McCarty, P. L.: *Environ. Eng. Div., ASCE.*, **107**(4), 831 (1981).
15. Kim, S. H.: Ph.D. Dissertation, University of Southern California, Los Angeles, California (1987).